Poultry Science®

Identification of central regulators related to abdominal fat deposition in chickens based on weighted gene co-expression network analysis

Wei Wei, Jiaxu Xiao, Najun Huang, Chaohui Xing, Jiangxian Wang, Xinxin He, Jinmei Xu, Hao Wang, Xing Guo, and Runshen Jiang[1]

College of Animal Science and Technology, Anhui Agricultural University, Hefei 230036, China

ABSTRACT Abdominal fat (**AF**) is one of the most important economic traits in chickens. Excessive AF in chickens will reduce feed utilization efficiency and negatively affect reproductive performance and disease resistance. However, the regulatory network of AF deposition needs to be further elucidated. In the present study, 300 one-day-old female Wannan chickens were reared to 17 wk of age, and 200 Wannan hens were selected to determine the abdominal fat percentage (**AFP**). Twenty AF tissue samples with the lowest AFP were selected as the low abdominal fat group (**L-AFG**), and 20 AF tissue samples with the highest AFP were selected as the high abdominal fat group (**H-AFG**). Eleven samples from L-AFG and 14 samples from H-AFG were selected for RNA-seq and used for weighted gene co-expression network analysis (**WGCNA**). Among the 25 RNA-seq samples, 5 samples with the lowest and highest AFP values were selected for differential expression gene analysis. Compared with the L-AFG, 225 and 101 genes were upregulated and downregulated in the H-AFG, respectively. A total of 20,503 genes were used to construct the WGCNA, and 44 co-expression gene modules were identified. Among these modules, 3 modules including turquoise, darkorange2, and floralwhite were identified as significantly associated with AFP traits. Furthermore, several genes including acyl-CoA oxidase 1 (***ACOX1***), stearoyl-CoA desaturase (***SCD***), aldehyde dehydrogenase 6 family member A1 (***ALDH6A1***), jun proto-oncogene, AP-1 transcription factor subunit (***JUN***), and fos proto-oncogene, AP-1 transcription factor subunit (***FOS***) involved in the "PPAR signaling pathway," "fatty acid metabolism," and "MAPK signaling pathway" were identified as central regulators that contribute to AF deposition. These results provide valuable information for further understanding of the gene expression and regulation of AF traits and contribute to future molecular breeding for AF in chickens.

Key words: chicken, abdominal fat, weighted gene co-expression network analysis, central regulator

2024 Poultry Science 103:103436
https://doi.org/10.1016/j.psj.2024.103436

INTRODUCTION

Fat is an important nutrient in the animal body, and the appropriate amount of fat deposition can improve meat quality and egg production traits (Chartrin et al., 2006; Zhao et al., 2007). With the improvement of genetic breeding, nutritional feed, and feeding management levels, excessive abdominal fat (**AF**) deposition has become more common in chickens. Excessive AF may lead to reduced feed conversion ratio, laying, fertility, and hatching rate (Zhang et al., 2017). Moreover, discarding excess AF will increase the amount of grease and waste in the treated water, causing environmental pollution. Therefore, it is essential to reveal the genetic basis contributing to AF deposition in order to implement effective genetic improvement programs.

Approximately 90% of fat is synthesized in the liver of poultry, where lipids are mainly produced as triglycerides (**TG**) (Hermier, 1997). TG is composed of glycerol and 3 molecular fatty acids. The main substrate of TG synthesis is fatty acids. For birds, de novo synthesis of fatty acids first uses glucose in the body through glycolysis and pyruvate decomposition to produce acetyl-CoA. Then acetyl-CoA carboxylase catalyzes the conversion of acetyl-CoA into malonyl-CoA, and second, malonyl-CoA is converted into fatty acid under the catalysis of fatty acid synthetase (Nematbakhsh et al., 2021). Over the past few decades, much research has been done on quantitative trait loci (**QTL**) and candidate genes associated with the AF traits in chickens. For example, QTL associated with AF deposition has been found on chromosome 7 in F2 populations derived from Satsumadori males and White Plymouth Rocks (Tatsuda and

Received November 11, 2023.
Accepted January 3, 2024.

[1]Corresponding author: jiangrunshen@ahau.edu.cn

Fujinaka, 2001). egl-9 family hypoxia inducible factor 1 (***EGLN1***), family with sequence similarity 120B (***FAM120B***), thrombospondin 2 (***THBS2***), and geranylgeranyl diphosphate synthase 1 (***GGPS1***) were found to be associated with AF deposition in the QTL region of chicken chromosome 3 (Moreira et al., 2015). Moreover, based on genome-wide association and mRNA expression analysis, it was revealed that several candidate genes are associated with AF traits in F2 populations derived from Beijing-You chickens and Cobb-Vantress, such as ret proto-oncogene (***RET***), collagen, type I, alpha 2 (***COL12A1***), vacuolar protein sorting-associated protein 4B (***VPS4B***), and forkhead box C1 (***FOXC1***) (Sun et al., 2013). With the rapid development of high-throughput sequencing technology, the weighted gene co-expression network analysis (**WGCNA**) method is now widely used in the study of histological analysis, and it is a powerful method to reveal the key regulatory genes, functional modules, and key nodes in the biological process of specific traits. By applying this approach, the genes fatty acid binding protein 1 (***FABP1***), ELOVL fatty acid elongase 6 (***ELOVL6***), and adiponectin, C1Q and collagen domain containing (***ADIPOQ***) were found to determine AF deposition in Wenchang chickens (Luo et al., 2022). The above studies show that AF is controlled by multiple genes and involves many regulatory networks. Despite many efforts, our understanding of how the regulatory network contributes to AF traits remains largely unknown and needs to be further illuminated.

Wannan Chicken is a well-known meat and egg dual-purpose chicken breed in Anhui Province, China. It is favored by consumers and producers because of its delicate meat quality, strong flavor, wide adaptability, and strong disease resistance (Jin et al., 2019). Moreover, AF deposition differs greatly among different individuals, which can be used as an excellent model to reveal the regulatory network of AF deposition and provide valuable resources for further study. In this study, we analyzed the gene expression profiles of AF tissue based on transcriptome data to study the difference in AF deposition in Wannan chickens, providing an important theoretical basis for AF deposition in chickens and molecular breeding.

MATERIALS AND METHODS

Experimental Birds and Sample Preparation

All bird-handling protocols were approved by the Animal Care and Use Committee of Anhui Agricultural University (Hefei, China) (permit number: SYXK (WAN) 2021−009). Three hundred 1-day-old female Wannan chickens were obtained from the Muzi Agricultural Development Co. Ltd., Anhui, China. All chickens were reared underlying a floor litter-rearing system. Stocking density (1−6 wk: 25 birds/m^2; 7−17 wk: 8 birds/m^2). The brooding temperature was maintained at 33 to 35°C for the first day and was gradually decreased by 2°C per week until 26°C and maintained at that level thereafter. From the starting period, 24 h of light were then reduced by 2 h per week until 12 h of light per day. The chickens were wing-banded and had ad libitum access to water and a pellet diet appropriate for the stage of development (1−3 wk: CP 17.5%, ME 11.59 MJ/kg; 4−17 wk: CP 15.5%, ME 10.98 MJ/kg). A total of 200 seventeen-wk-old Wannan hens were selected. After fasting for 12 h, body weight and wing number were recorded and then euthanized by electrical stunning followed by exsanguination. AF was quickly dissected and weighed; a sample was immediately snap-frozen in liquid nitrogen and stored at −80° C until further processing. Abdominal fat percentage (**AFP**) was calculated as a percentage of AF weight to live weight. Twenty AF tissue samples with the lowest AFP were selected as the low abdominal fat group (**L-AFG**), and 20 AF tissue samples with the highest AFP were selected as the high abdominal fat group (**H-AFG**).

RNA Extraction and Sequencing

Eleven samples from L-AFG and 14 samples from H-AFG were selected for RNA-seq. Total RNA was extracted from 25 AF tissue samples by using TRIzol reagent (Invitrogen, Carlsbad, CA) following the manufacturer's protocol. The RNA integrity and concentration were measured by the Agilent Bioanalyzer 2,100 system (Agilent Technologies, Santa Clara, CA) and using a NanoDrop spectrophotometer 2000 (Thermo Scientific, Wilmington, DE). A total of 25 RNA libraries were constructed with the mRNA-Seq Sample Preparation Kit (Illumina, San Diego, CA), according to the manufacturer's instructions. Qualified libraries were uploaded on the Illumina NovaSeq 6000 platform for sequencing with a read length of PE150. Accession to cite for these SRA data is PRJNA1034014.

Analysis of Differentially Expressed Genes

Read quality control was performed using Trim_Galore (https://github.com/FelixKrueger/Tri-mGalore/) with the parameters "-q 20 −phred33 −stringency 3 −paired." Use HISAT2 (Kim et al., 2019) to align the trimmed reads to a reference genome (GRCg6a). The BAM files were sorted and indexed using Samtools (Li et al., 2009). Readings for each gene were tallied using the htseq-count script in Python (Anders et al., 2015).

Among the 25 samples used for RNA-seq, 5 samples with the highest AFP and 5 samples with the lowest AFP were selected for AF tissue differentially expressed genes (**DEG**) analysis. The analysis of differentially expressed transcripts was performed with the DESeq2 R package (v 4.2.2) (Love et al., 2014), which was defined as genes with a false discovery rate (padj) ≤ 0.05 and a $|\log2(\text{fold change})| \geq 1$. The volcano plot was used to visualize the overall distribution of DEG.

Weighted Gene Co-Expression Network Analysis

Gene expression level normalization was performed by the "variance-stabilizing Transformation" function of DESeq2 (Love et al., 2014). The WGCNA was performed using the WGCNA package (v1.7.1) (Langfelder and Horvath, 2008) in R software. Firstly, the Pearson correlation between genes was calculated to construct a gene co-expression correlation matrix. Subsequently, a soft threshold ($\beta = 3$) conforming to the scale-free network construction was selected to generate a weighted adjacency matrix. Furthermore, the adjacency matrix can be converted into a topological overlap matrix (**TOM**), and the corresponding difference degree (1-TOM) can be calculated. The module is divided according to the dynamic TreeCut standard, the minimum capacity of the module is set to 30 and the shear height of the module is set to 0.3 with 1-TOM as the measurement value. Finally, the phenotype data related to AFP and gene modules were quantified using Pearson correlation. Hub genes were filtered with module membership (**MM**) > 0.8 and gene significance (**GS**) > 0.4. Hub genes were overlapped with DEG, and the overlapping genes were identified as central regulators.

The protein−protein interaction (**PPI**) network of the hub genes was analyzed using the STRING database (Szklarczyk et al., 2023), where the minimum required interaction score was set to high confidence (0.700). The PPI network for the hub genes was visualized with Cytoscape (v3.10.0) (Shannon et al., 2003). The calculation of transcripts per million (**TPM**) was performed by TPMCalculator software to quantify the expression levels of central regulators (Vera Alvarez et al., 2019).

Functional Enrichment Analysis

Gene Ontology (**GO**) enrichment analysis of genes was performed using an online annotation tool g: Profiler (Reimand et al., 2016). The GO terms with a Benjamini-Hochberg FDR P-value of 0.05 were considered as the significance threshold to identify the functional categories. Kyoto Encyclopedia of Genes and Genomes (**KEGG**) pathway enrichment analysis was performed using KOBAS version 3.0 (Bu et al., 2021). The significance level for KEGG pathways was set to $P < 0.05$.

Quantitative Real-Time PCR Analysis

10 samples from each of the L-AFG and H-AFG of Wannan chickens were selected for quantitative real-time PCR (**qPCR**) analysis. To verify whether the central regulators were associated with the AF traits in the other breeds, we selected 100 ninety-day-old Huainan chickens to determine the AFP value, and based on the AFP value, 5 AF tissue samples with the lowest AFP and 5 AF tissue samples with the highest AFP were selected for qPCR analysis (Table S1). Total RNA was extracted using TRIzol (Invitrogen) according to the instructions. cDNA was synthesized by reverse transcription kit (Vazyme, Nanjing, China). Primer 6.0 was used to design the mRNA primers (Table S2). The qPCR was performed using an ABI Prism 7500 instrument (Applied Biosystems, Carlsbad, CA) using SYBR Green Supermix (Vazyme), with *GAPDH* as an internal reference, and 3 replicates for each sample. The relative expression of mRNA was calculated using the $2^{-\Delta\Delta Ct}$ method (Vandesompele et al., 2002).

Statistical Analysis

The AFP was analyzed by SPSS version 26.0 software (SPSS Inc., Chicago, IL). We used the Student's t-test to assess the significance of the difference between L-AFG and H-AFG means. The threshold for significance was set at $P < 0.05$. Data are expressed as mean ± SD. Pearson correlation coefficient analysis was conducted between the results of qPCR and RNA-seq.

RESULTS

The AFP of Wannan Chickens

The AFP in the H-AFG and L-AFG of Wannan chickens is shown in Table 1. The AFP of H-AFG was 2.74% higher than that of L-AFG ($P < 0.001$) (Table 1).

Transcriptome Profiles

A total of 25 libraries were sequenced, and a total of 565.61 MB clean reads were obtained. The average output of each sample is 6.76 GB of data, the minimum data volume of 25 samples is 5.87 GB, and the maximum data volume is 7.74 GB. The average ratio of Q20 is 98.08%, and the average ratio of Q30 is 95.02%. The GC content of the 25 samples ranged from 48.83% to 50.06% (Table S3). In total, 23,239 genes were detected in Wannan chicken AF tissues, and the number of expressed genes in each library ranged from 17,933 to 21,430 (Table S4).

GO Enrichment Analysis of DEG

Among the 25 samples used for RNA-seq, 5 samples with the highest AFP and 5 samples with the lowest AFP were selected for AF tissue DEG analysis (Table S5). The DEG between the H-AFG and L-AFG are shown in the volcano plot (Figure 1A). Compared to

Table 1. Comparison of AFP between L-AFG and H-AFG of Wannan chickens.

Item	AFP
L-AFG	0.45 ± 0.20
H-AFG	$3.19 \pm 0.98^{***}$

Abbreviations: AFP, abdominal fat percentage; H-AFG, high abdominal fat group; L-AFG, low abdominal fat group.

The data are presented as mean ± SD ($n = 20$) ($^{***}P < 0.001$).

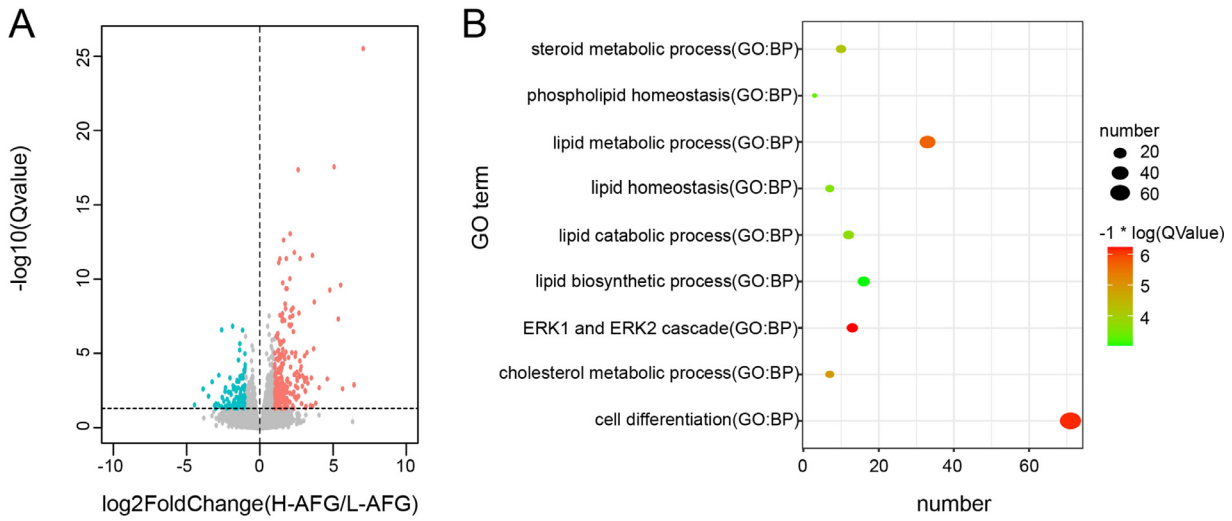

Figure 1. (A) Volcano plot for H-AFG vs. L-AFG DEG. (B) GO functional enrichment analysis of DEG in abdominal fat. L-AFG means low abdominal fat group, H-AFG means high abdominal fat group, and DEG means differentially expressed genes.

the L-AFG, 225 and 101 genes were upregulated and downregulated in the H-AFG. GO analysis showed that DEG were enriched in 137 biological processes including "lipid metabolic process," "cholesterol metabolic process," "lipid catabolic process," "lipid homeostasis," etc. (Table S6 and Figure 1B).

Weighted Gene Co-Expression Network Construction and Module Detection

To explore the hub genes that are involved in regulating AF traits in Wannan chickens, a total of 20,503 genes were obtained to build the weighted gene co-expression network. Based on sample clustering information, no outlier samples were found (Figure 2A). After determining a soft threshold at $R^2 > 0.85$ (Figure 2B). Following the dynamic tree cut, 44 co-expression gene modules were identified, palevioletred3 contains the least number of genes at 60, and turquoise contains the most at 3,955 (Figure 2C and Table S7). In addition, we draw a heat map based on the correlation between eigengenes. It shows the degree of correlation between eigengenes of different modules (Figure 2D).

Identification of Modules Associated With AFP Traits

To identify co-expression modules associated with traits of AFP, we evaluated the relationship of AFP to module eigengene (**ME**) (Figure 3). AFP was significantly and positively correlated with the grey60 module ($r = 0.53$, $P = 0.006$), turquoise module ($r = 0.81$, $P = 8 \times 10^{-7}$), darkgray module ($r = 0.47$, $P = 0.02$), and darkorange2 module ($r = 0.73$, $P = 4 \times 10^{-5}$). Significant negative correlations were found with the pink module ($r = -0.52$, $P = 0.008$), floralwhite module ($r = -0.71$, $P = 8 \times 10^{-5}$), and ivory module ($r = -0.61$, $P = 0.001$). At the same time, we focus on modules with absolute correlation values greater than 0.7 with AFP traits. In the present study, we focus on turquoise, darkorange2, and floralwhite module.

Identification and GO Analysis of Hub Genes in the Correlation Module

After identifying the 3 correlation modules, hub genes were filtered with GS > 0.4 and MM > 0.8. The turquoise module obtained 251 hub genes (Table S8), and the correlation between GS and MM was 0.82 ($P < 1e\text{-}200$) (Figure 4A). Functional enrichment analysis showed that hub genes in this module were significantly enriched in GO terms such as "lipid metabolic process," "fatty acid metabolic process," and "glycerol-3-phosphate metabolic process" (Figure 4B and Table S9). The darkorange2 module obtained 19 hub genes (Table S8), and the correlation between GS and MM was 0.76 ($P = 1.1e\text{-}91$) (Figure 4C). The hub genes in this module were significantly enriched in GO terms such as "insulin-like growth factor receptor binding," "regulation of lipid metabolic process," and "regulation of lipid biosynthetic process" (Figure 4D and Table S9). The floralwhite module obtained 6 hub genes (Table S8), and the correlation between GS and MM was 0.76 ($P = 3.3e\text{-}24$) (Figures 4E). Hub genes were significantly enriched in such GO terms as "glycosaminoglycan binding," "acetylcholine receptor regulator activity," and "extracellular matrix" (Figure 4F and Table S9).

KEGG Pathway Enrichment Analysis of Central Regulators in the Correlation Module

We overlapped the hub genes and DEG, resulting in 77 upregulated genes in the turquoise module, 8 upregulated genes in the darkorange2 module, and 3 downregulated genes in the floralwhite module being identified as central regulators (Table S10). We analyzed these central regulators separately for KEGG pathway enrichment. In the turquoise module, 7 pathways were

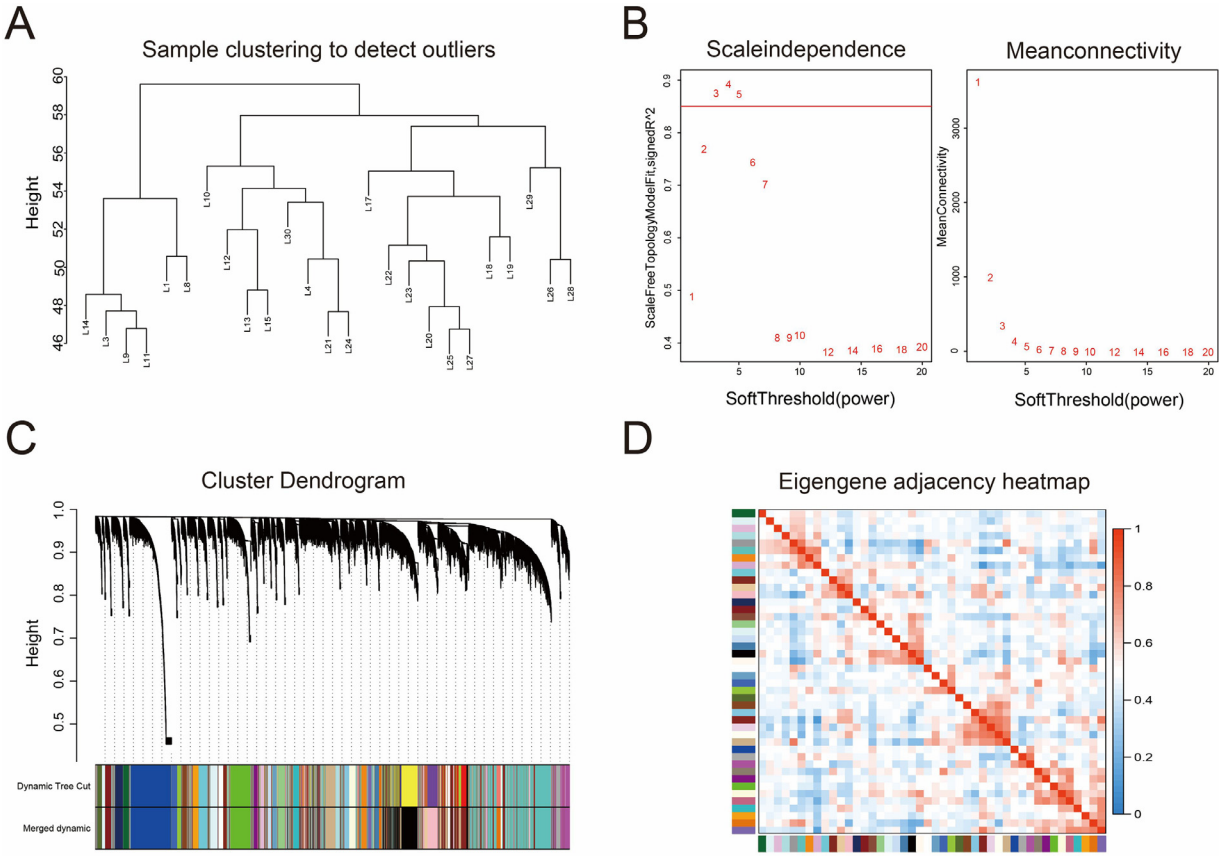

Figure 2. (A) Sample clustering. (B) Scale independence and mean connectivity. (C) The cluster of genes. (D) Eigengene adjacency heatmap: Colors in the eigengene adjacency heatmap indicate the intensity of correlations. The redder the colors are, the stronger the correlations are.

significantly enriched, among which "PPAR signaling pathway," "Wnt signaling pathway," "fatty acid metabolism," "biosynthesis of unsaturated fatty acids," "propanoate metabolism," and "beta-alanine metabolism" were possibly necessary for AF deposition (Figure 5A and Table S11). In addition, in the darkorang2 module, 10 pathways are significantly enriched, such as "GnRH signaling pathway," "Toll-like receptor signaling pathway," "apoptosis," and "MAPK signaling pathway" (Figure 5B and Table S12). However, no pathways were significantly enriched in the floralwhite module.

PPI of Hub Genes in the Correlation Module

The PPI analysis of hub genes was conducted using the STRING database and visualized using Cytoscape (v3.10.0) (Figure 6). Through PPI analysis, protein interactions were identified in the central regulators acyl-CoA oxidase 1 (***ACOX1***), stearoyl-CoA desaturase (***SCD***), and aldehyde dehydrogenase 6 family member A1 (***ALDH6A1***) within the turquoise module (Figure 6A). Within the darkorange2 module, protein interactions were observed among the central regulators early growth response 1 (***EGR1***), early growth response 2 (***EGR2***), early growth response 4 (***EGR4***), cysteine-rich angiogenic inducer 61 (***CYR61***), BTG anti-proliferation factor 2 (***BTG2***), jun proto-oncogene, AP-1 transcription factor subunit (***JUN***) and fos proto-oncogene, AP-1 transcription factor subunit (***FOS***) (Figure 6B). No gene protein interaction was found in the floralwhite module.

Expression Levels of Central Regulators in the Correlation Module

We further quantified the expression levels of central regulators in correlation modules using log (1+TPM) values. There was a significant difference in the expression level of central regulators in the samples L-AFG and H-AFG. Most of the central regulators in the turquoise module, including *ACOX1* and *SCD* were abundantly expressed in the H-AFG of Wannan chickens (Figure 7). In the darkorange2 module, *JUN, EGR1, FOS*, and *CYR61* were highly expressed (Figure S1). However, all central regulators of the floralwhite module were expressed at low to moderate levels in the H-AFG of Wannan chickens (Figure S2).

Verification of Expression Levels of Genes

To verify the expression levels of genes, the fold change of L-AFG and H-AFG measured by qPCR were compared with those measured by RNA-seq. The results of the 12 selected genes in RNA-seq and qPCR showed a similar trend (Figure 8A). Pearson correlation coefficient analysis was conducted between the results of qPCR and RNA-seq using SPSS software, and the correlation coefficient was 0.98 (Figure 8B). To determine if

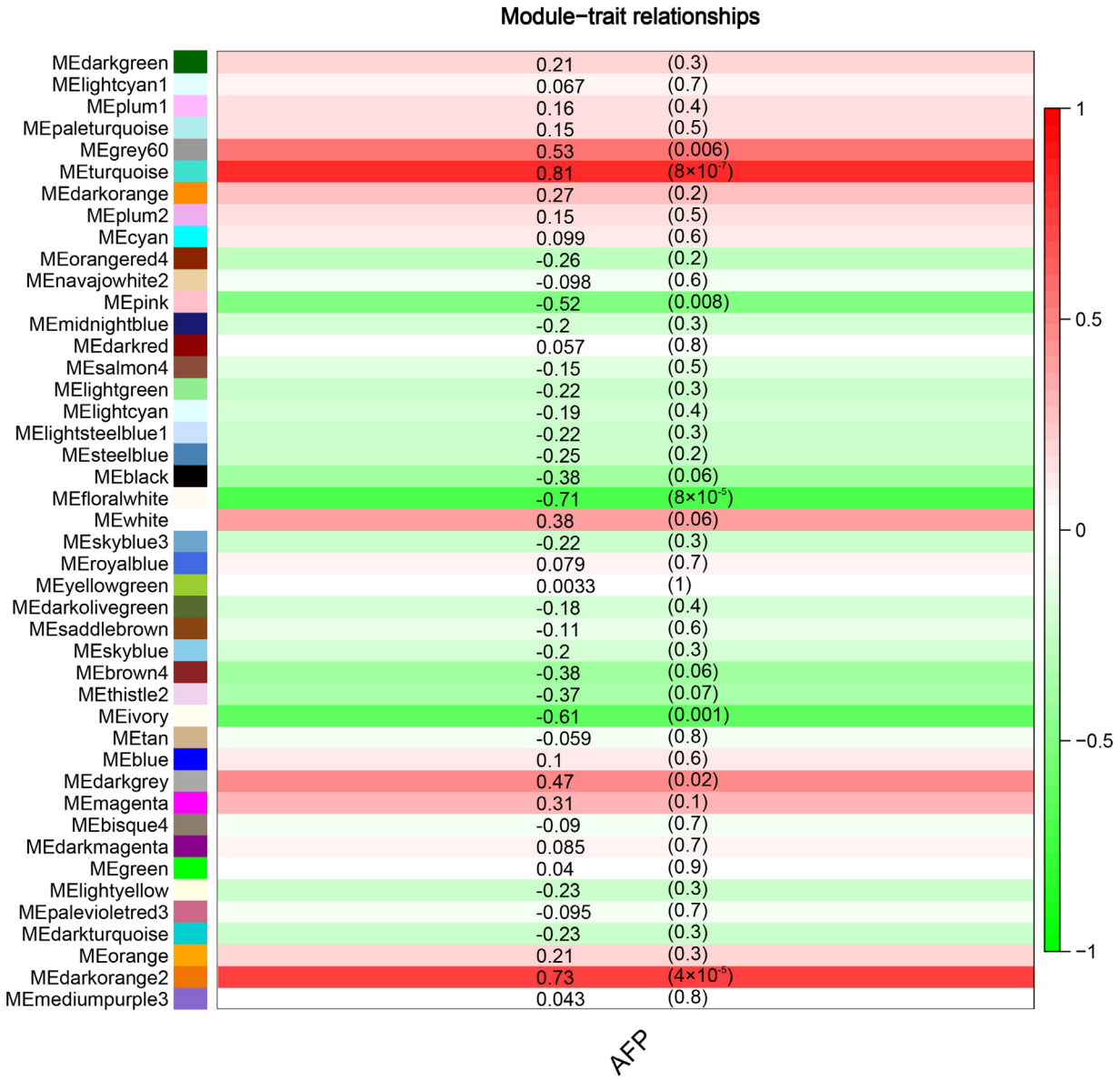

Figure 3. Module−trait relationships. Each row represents a different module obtained from the WGCNA, and each column corresponds to a trait. Each cell contains the correlation and *P*-value associated with the relationship. AFP means abdominal fat percentage and ME means module eigengene.

the central regulators were linked to AF traits in other breeds, we conducted qPCR validation on AF in Huainan chickens. The study results indicate that 6 central regulators (*ACOX1, ALDH6A1, JUN, EGR1, FOS*, and *SCD*) were expressed at higher levels in H-AFG compared to L-AFG (Figure S3).

DISCUSSION

Abdominal fat is one of the most important economic traits in chickens. It is known that AF deposition in chickens depends on the balance of lipid synthesis, transport, uptake, and subsequent metabolism, which involves many genes and pathways. Therefore, revealing the regulatory network of AF deposition in chickens at the level of gene co-expression is of great significance for studying the mechanism of AF deposition. In this study, DEG and WGCNA analysis were used to identify specific expressed genes and signaling pathways involved in AF deposition.

Based on the DEG, the results of GO analysis showed that DEG from AF tissues were enriched in 137 biological processes. Among them, 24-dehydrocholesterol reductase (***DHCR24***), nuclear factor, erythroid 2 like 1 (***NFE2L1***), insulin induced gene 2 (***INSIG2***), hydroxysteroid 17-beta dehydrogenase 7 (***HSD17B7***), cytochrome P450 family 39 subfamily A member 1 (***CYP39A1***), apolipoprotein A1 (***APOA1***), and fibroblast growth factor 1 (***FGF1***) play an essential role in the "lipid metabolic process," "cholesterol metabolic process," "lipid catabolic process," and "lipid homeostasis." *DHCR24* and *HSD17B7* are steroid biosynthesis genes, and up-regulation of steroid biosynthesis genes can increase fat accumulation in chickens (Mu et al., 2019). *NFE2L1* belongs to the CNC-bZIP family, which plays

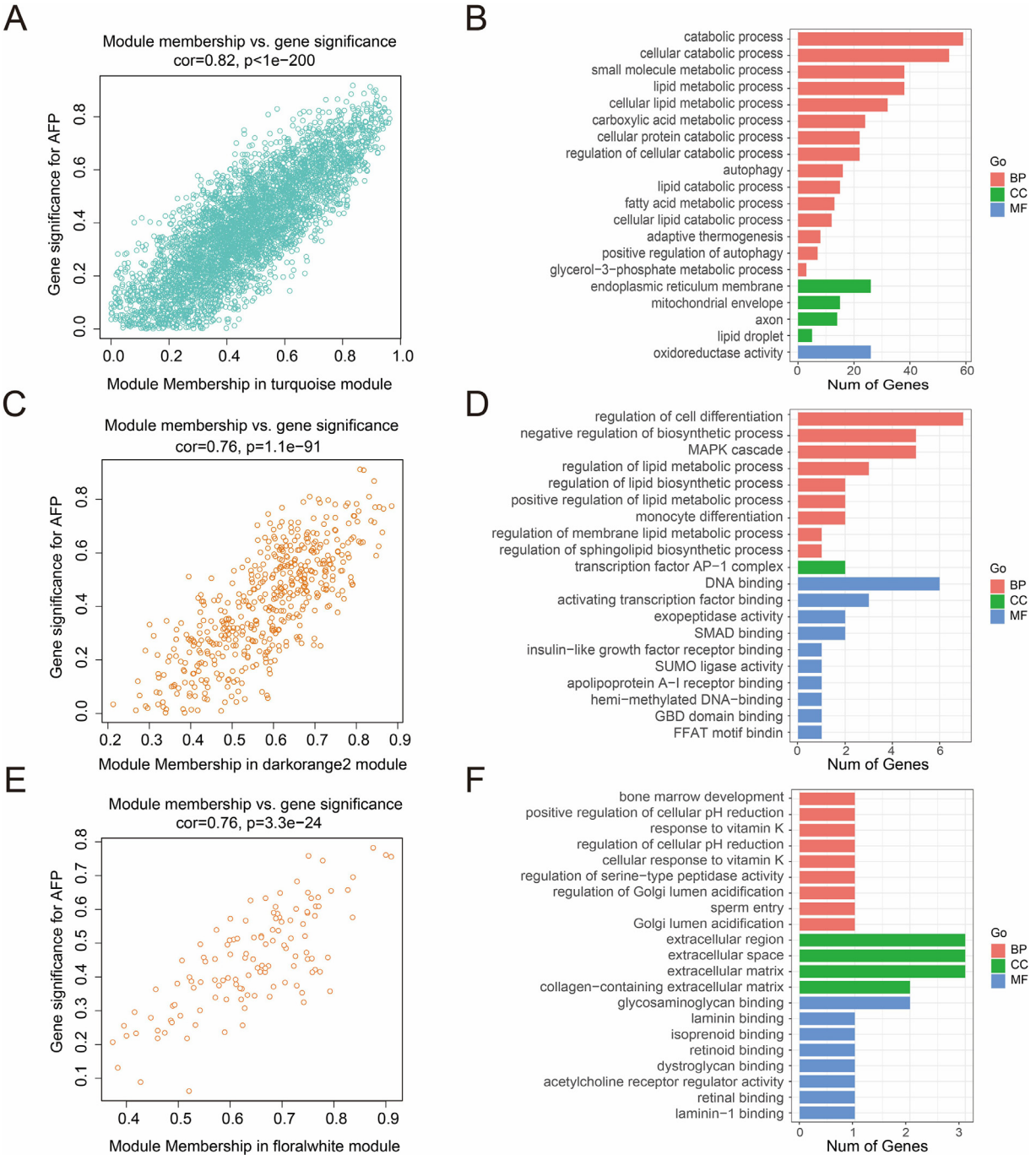

Figure 4. Hub genes screening and functional analysis in turquoise, darkorange2, and floralwhite modules. Scatter plot of gene significance and module membership for (A) turquoise module, (C) darkorange2 module, and (E) floralwhite module. GO functional enrichment analysis of hub genes in (B) turquoise module, (D) darkorange2 module, and (F) floralwhite module.

a key role in regulating glucose metabolism, mitochondrial function, and insulin secretion (Zheng et al., 2015). Studies have shown that the deficiency of *NFE2L1* affects adipogenesis and adipose tissue function (Ren et al., 2021). *INSIG2* is involved in the regulation of cholesterol metabolism and lipogenesis in mammals (Fan et al., 2021). *CYP39A1* plays a key role in removing cholesterol and inhibiting liver sterol accumulation (de Boer et al., 2018). *APOA1* may be associated with tissue-specific fat deposition in chickens (Zhang et al., 2019). *FGF1* is an autocrine/paracrine regulator that plays a key role in the development, structural, and metabolic remodeling of adipose tissue (Zhang et al., 2018). These DEG and categories may play an important role in the accumulation of AF in chickens.

According to the correlation between phenotypes and gene expression levels based on weighted gene co-expression networks, turquoise and darkorange2 modules are concerned. This could effectively explain how these modules may potentially determine the amount of AF deposition. By aggregating the hub genes in the correlation modules and analyzing them in conjunction with the DEG, central regulators that play an important role in AF deposits can be further identified.

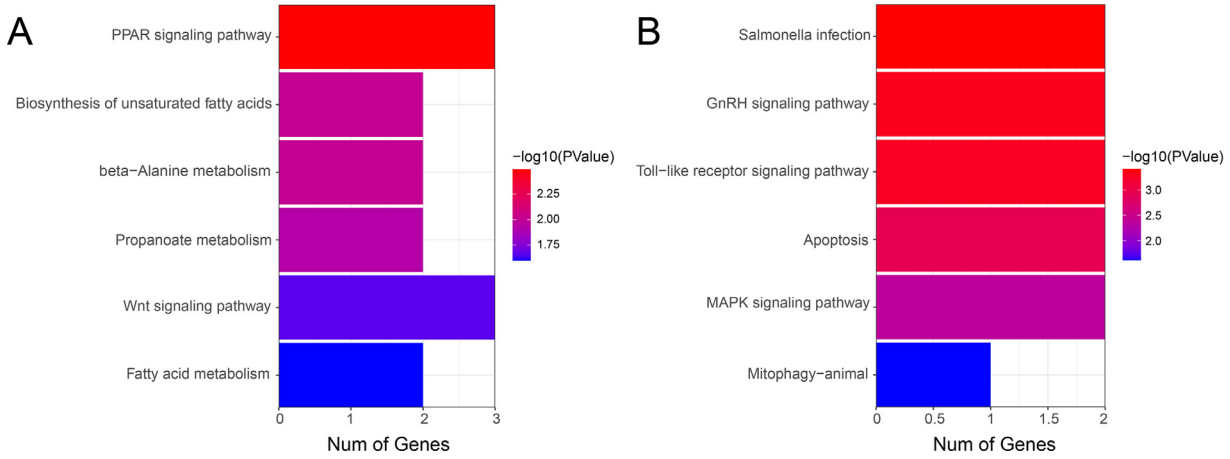

Figure 5. KEGG pathways enrichment analysis of central regulators in (A) turquoise module and (B) darkorange2 module.

In the turquoise module, central regulators were significantly enriched in pathways related to "PPAR signaling pathway," "Wnt signaling pathway," "fatty acid metabolism," "biosynthesis of unsaturated fatty acids," "propanoate metabolism," and "beta-alanine metabolism." *ACOX1* and *SCD* are significantly enriched in the "PPAR signaling pathway," "fatty acid metabolism," and "biosynthesis of unsaturated fatty acids." *ACOX1* is the first rate-limiting enzyme in peroxisome fatty acid beta-oxidation, which promotes adipogenesis in bovine intramuscular preadipocytes by regulating peroxisome fatty acid beta-oxidation (Zhang et al., 2021). Also in chickens, studies have shown that the regulation of *ACOX1* can reduce fatty acid oxidation and promote the differentiation of chicken intramuscular preadipocytes (Li et al., 2019). It is worth noting that *SCD* has the largest fold change in DEG. *SCD* is a key enzyme in the de novo synthesis of fatty acids. *SCD* is located downstream of fatty acid synthase (***FASN***) during de novo fatty acid synthesis and catalyzes the conversion of saturated fatty acid to monounsaturated fatty acid (Liu et al., 2010; von Roemeling et al., 2015). It was reported that *SCD* is enriched in the "PPAR signaling pathway" in Wenchang chickens AF (Luo et al., 2022), this is consistent with the results of this study. In addition, *ACOX1* and *ALDH6A1* are significantly enriched in "beta-alanine metabolism" and "propanoate metabolism." Some studies have shown that beta-alanine can increase carnosine content (Stegen et al., 2014). Lee et al. found that insulin levels increased significantly after carnosine ingestion in diabetic mice (Lee et al., 2005). *ALDH6A1* is reported to convert malondialdehyde into acetyl-CoA, a carbon source for fatty acid synthesis, cholesterol synthesis, and ketone formation (Yang et al., 2021). It can be seen from the above that "beta-alanine metabolism" and "propanoate metabolism" may play an important role in AF deposition.

In the darkorange2 module, central regulators were significantly enriched in pathways related to the "GnRH signaling pathway," "Toll-like receptor signaling pathway," "apoptosis," and "MAPK signaling pathway." Among them, JUN and FOS were significantly enriched in the "Toll-like receptor signaling pathway," "apoptosis," and "MAPK signaling pathway." Toll-like receptors

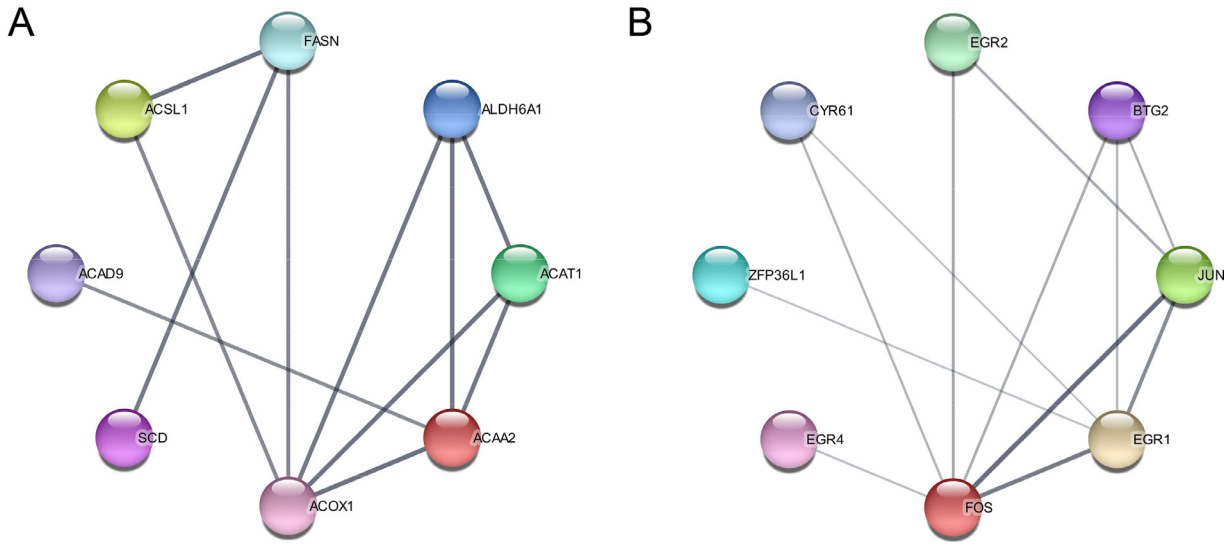

Figure 6. (A) PPI network of the hub genes in the turquoise module. (B) PPI network of the hub genes in the darkorange2 module. The thickness of the line between 2 nodes reflects the strength of the protein interaction.

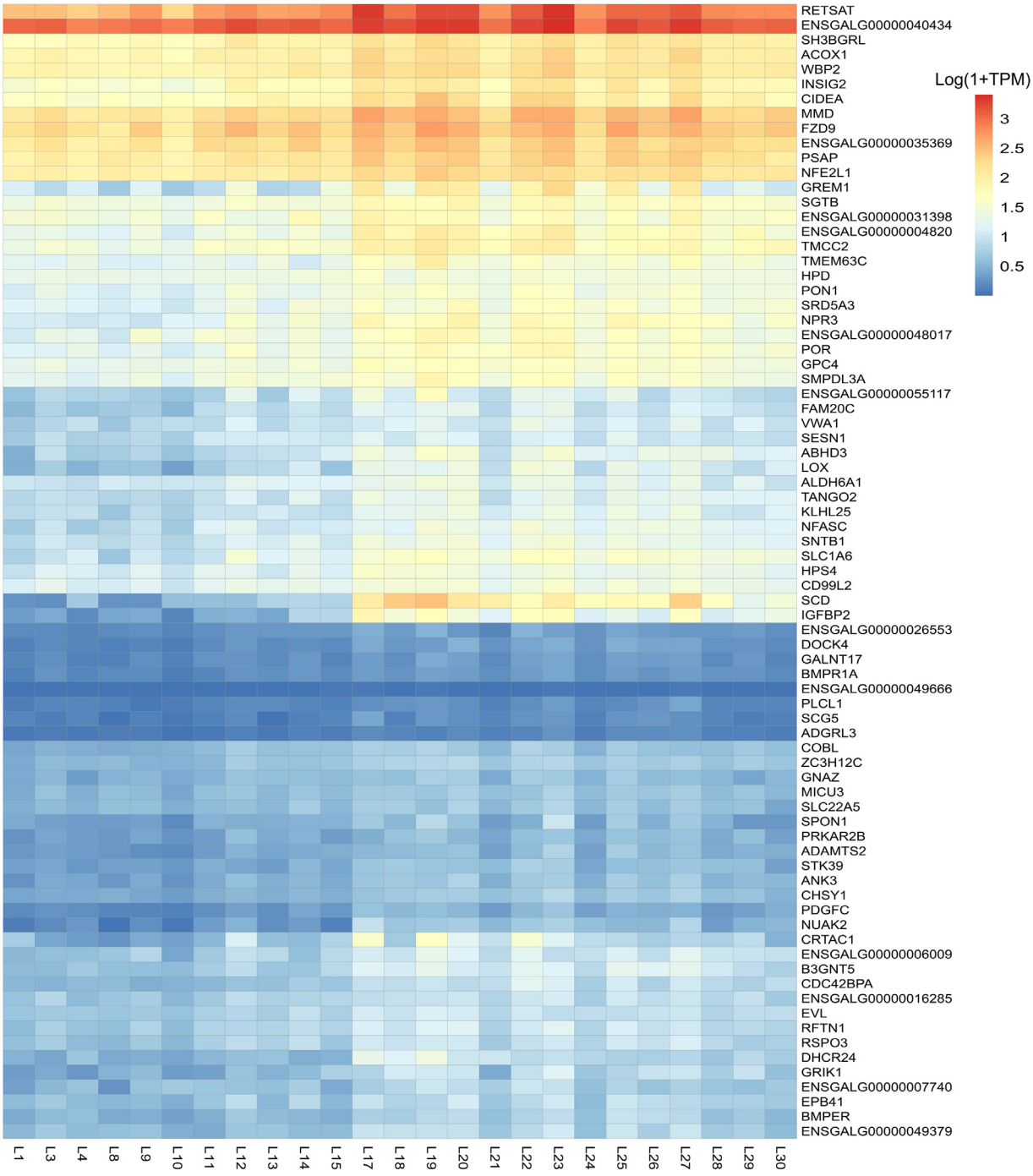

Figure 7. Expression of the central regulators in the L-AFG (L1−L15) and H-AFG (L17−L30) in the turquoise module. Each row represents a different sample and each column corresponds to a gene. Each cell contains the expression of the gene in the sample. L-AFG means low abdominal fat group, and H-AFG means high abdominal fat group.

(**TLRs**) have been identified as dominant innate immune receptors (Shafeghat et al., 2022), which play a central role in the development and function of the immune system (Aluri et al., 2021). Studies have shown that TLR4 can activate "MAPK signaling pathways" (Li et al., 2022). MAPK pathway regulates the expression of fat transcription factors during adipogenesis (Aouadi et al., 2006). *JUN* and *FOS* are subunits of activating protein-1 transcription factors, and *FOS* has been reported to be involved in various cellular changes. It is involved in the synthesis of cholesterol (Choi et al., 2021). It was reported that *JUN* could increase lipid accumulation by activating the transcription of sterol regulatory element binding transcription factor 1 (Guo et al., 2016). It can be seen that *JUN* and *FOS* may indirectly or directly affect AF deposition in chickens. In addition, *JUN* and *EGR1* are significantly enriched in the "GnRH signaling pathway." GnRH can be stimulated and released by leptin (Zieba et al., 2005). Moreover, the expression of leptin in fully fed animals reflects adipocyte size and body-fat mass (Houseknecht and Portocarrero, 1998), and leptin binds to its specific receptors to activate the MAPK pathway (Herrera-Vargas et al., 2021). *EGR1* is a transcription factor significantly

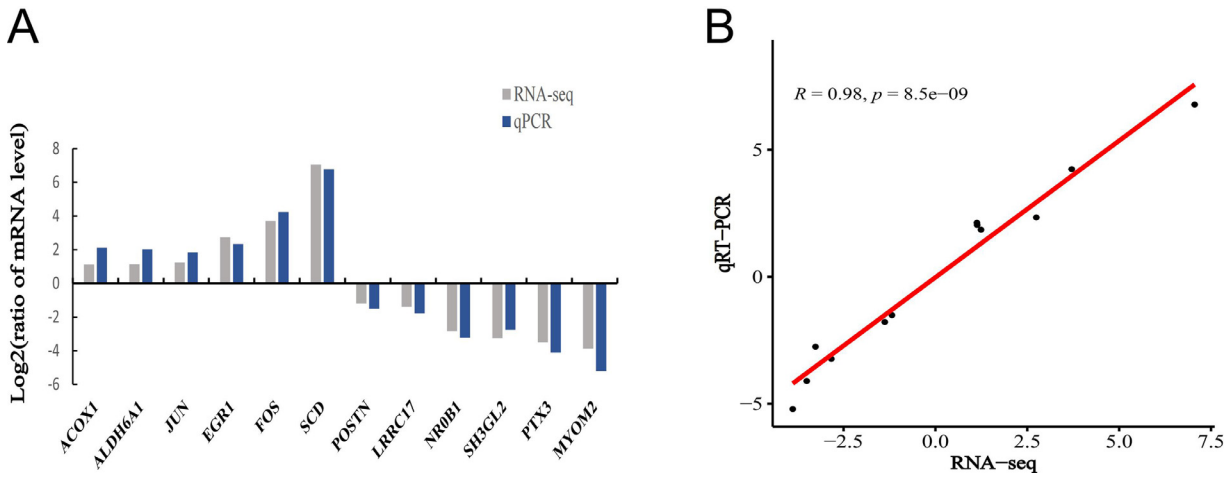

Figure 8. (A) Comparisons between qPCR and RNA-seq measurements of the expression abundance of 12 genes. (B) Correlations of the mRNA expression levels of 12 genes based on RNA-seq and qPCR analyses.

induced by insulin and nutrients in adipocytes, which not only mediates the effect of insulin on the production of lipolysis but also coordinates the action of insulin with the endogenous circadian rhythm of adipose tissue (Meriin et al., 2022).

With the continuous advancement of technology, molecular marker-assisted breeding has become one of the technologies that have attracted attention and application in the field of poultry production. This technology utilizes molecular marker techniques and genetic principles to rapidly and accurately screen poultry breeds with desirable genetic traits, avoiding the time-consuming breeding process and lengthy feeding cycles associated with traditional breeding methods (Zhou et al., 2023). The present study may provide promising genes for applying this technique in poultry breeding for AF trait selection.

CONCLUSIONS

In the present study, we provided a useful resource of gene expression data for chicken AF tissue development. The results showed that central regulators *ACOX1, SCD, ALDH6A1, JUN, FOS, EGR1*, and other potentially detected genes could further inform selection for the AF trait.

ACKNOWLEDGMENTS

This work was supported by the Science and Technology Major Project of Anhui Province (202203a06020015); the Key Research and Development Project of Anhui Province (202204c06020050); the Science and Technology Major Project of Huaibei City (HK2021015); the Natural Science Research Project of Anhui Educational Committee (KJ2021A0148); and the China Agriculture Research System of MOF and MARA (CARS-41).

DISCLOSURES

The authors confirm that there are no conflicts of interest.

SUPPLEMENTARY MATERIALS

Supplementary material associated with this article can be found in the online version at doi:10.1016/j.psj.2024.103436.

REFERENCES

Aluri, J., M. A. Cooper, and L. G. Schuettpelz. 2021. Toll-like receptor signaling in the establishment and function of the immune system. Cells 10:1374.

Anders, S., P. T. Pyl, and W. Huber. 2015. HTSeq−a Python framework to work with high-throughput sequencing data. Bioinformatics 31:166–169.

Aouadi, M., K. Laurent, M. Prot, Y. L.e Marchand-Brustel, B. Binétruy, and F. Bost. 2006. Inhibition of p38MAPK increases adipogenesis from embryonic to adult stages. Diabetes 55:281–289.

Bu, D., H. Luo, P. Huo, Z. Wang, S. Zhang, Z. He, Y. Wu, L. Zhao, J. Liu, J. Guo, S. Fang, W. Cao, L. Yi, Y. Zhao, and L. Kong. 2021. KOBAS-i: intelligent prioritization and exploratory visualization of biological functions for gene enrichment analysis. Nucleic Acids Res. 49:W317–W325.

Chartrin, P., K. Méteau, H. Juin, M. D. Bernadet, G. Guy, C. Larzul, H. Rémignon, J. Mourot, M. J. Duclos, and E. Baéza. 2006. Effects of intramuscular fat levels on sensory characteristics of duck breast meat. Poult. Sci. 85:914–922.

Choi, Y., H. Jeon, J. W. Akin, T. E. Curry, and M. Jo. 2021. The FOS/AP-1 regulates metabolic changes and cholesterol synthesis in human periovulatory granulosa cells. Endocrinology 162: bqab127.

de Boer, J. F., F. Kuipers, and A. K. Groen. 2018. Cholesterol transport revisited: a new turbo mechanism to drive cholesterol excretion. Trends Endocrinol. Metab. 29:123–133.

Fan, X., Y. Zhang, L. Qiu, and Y. Miao. 2021. Negative effect of insulin-induced gene 2 on milk fat synthesis in buffalo mammary epithelial cells. J. Dairy Res. 88:401–406.

Guo, J., W. Fang, L. Sun, Y. Lu, L. Dou, X. Huang, M. Sun, C. Pang, J. Qu, G. Liu, and J. Li. 2016. Reduced miR-200b and miR-200c expression contributes to abnormal hepatic lipid accumulation by stimulating JUN expression and activating the transcription of srebp1. Oncotarget 7:36207–36219.

Hermier, D. 1997. Lipoprotein metabolism and fattening in poultry. J. Nutr. 127:805s–808s.

Herrera-Vargas, A. K., E. García-Rodríguez, M. Olea-Flores, M. A. Mendoza-Catalán, E. Flores-Alfaro, and N. Navarro-Tito. 2021. Pro-angiogenic activity and vasculogenic mimicry in the tumor microenvironment by leptin in cancer. Cytokine Growth Factor Rev. 62:23–41.

Houseknecht, K. L., and C. P. Portocarrero. 1998. Leptin and its receptors: regulators of whole-body energy homeostasis. Domest. Anim. Endocrinol. 15:457–475.

Jin, S., X. Fan, L. Yang, T. He, Y. Xu, X. Chen, P. Liu, and Z. Geng. 2019. Effects of rearing systems on growth performance, carcass yield, meat quality, lymphoid organ indices, and serum biochemistry of Wannan Yellow chickens. Anim. Sci. J. 90:887–893.

Kim, D., J. M. Paggi, C. Park, C. Bennett, and S. L. Salzberg. 2019. Graph-based genome alignment and genotyping with HISAT2 and HISAT-genotype. Nat. Biotechnol. 37:907–915.

Langfelder, P., and S. Horvath. 2008. WGCNA: an R package for weighted correlation network analysis. BMC Bioinf. 9:559.

Lee, Y. T., C. C. Hsu, M. H. Lin, K. S. Liu, and M. C. Yin. 2005. Histidine and carnosine delay diabetic deterioration in mice and protect human low density lipoprotein against oxidation and glycation. Eur. J. Pharmacol. 513:145–150.

Li, B., M. Wang, S. Chen, M. Li, J. Zeng, S. Wu, Y. Tu, Y. Li, R. Zhang, F. Huang, and X. Tong. 2022. Baicalin mitigates the neuroinflammation through the TLR4/MyD88/NF-κB and MAPK pathways in LPS-stimulated BV-2 microglia. Biomed. Res. Int. 2022:3263446.

Li, G., S. Fu, Y. Chen, W. Jin, B. Zhai, Y. Li, G. Sun, R. Han, Y. Wang, Y. Tian, H. Li, and X. Kang. 2019. MicroRNA-15a regulates the differentiation of intramuscular preadipocytes by targeting ACAA1, ACOX1 and SCP2 in chickens. Int. J. Mol. Sci. 20:4063.

Li, H., B. Handsaker, A. Wysoker, T. Fennell, J. Ruan, N. Homer, G. Marth, G. Abecasis, and R. Durbin. 2009. The Sequence alignment/map format and SAMtools. Bioinformatics 25:2078–2079.

Liu, X., M. Miyazaki, M. T. Flowers, H. Sampath, M. Zhao, K. Chu, C. M. Paton, D. S. Joo, and J. M. Ntambi. 2010. Loss of stearoyl-CoA desaturase-1 attenuates adipocyte inflammation: effects of adipocyte-derived oleate. Arterioscler. Thromb. Vasc. Biol. 30:31–38.

Love, M. I., W. Huber, and S. Anders. 2014. Moderated estimation of fold change and dispersion for RNA-seq data with DESeq2. Genome Biol. 15:550.

Luo, N., J. Shu, X. Yuan, Y. Jin, H. Cui, G. Zhao, and J. Wen. 2022. Differential regulation of intramuscular fat and abdominal fat deposition in chickens. BMC Genomics 23:308.

Meriin, A. B., N. Zaarur, D. Roy, and K. V. Kandror. 2022. Egr1 plays a major role in the transcriptional response of white adipocytes to insulin and environmental cues. Front. Cell. Dev. Biol. 10:1003030.

Moreira, G. C., T. F. Godoy, C. Boschiero, A. Gheyas, G. Gasparin, S. C. Andrade, M. Paduan, H. Montenegro, D. W. Burt, M. C. Ledur, and L. L. Coutinho. 2015. Variant discovery in a QTL region on chromosome 3 associated with fatness in chickens. Anim. Genet. 46:141–147.

Mu, X., X. Cui, R. Liu, Q. Li, M. Zheng, G. Zhao, C. Ge, J. Wen, Y. Hu, and H. Cui. 2019. Identification of differentially expressed genes and pathways for abdominal fat deposition in ovariectomized and sham-operated chickens. Genes (Basel) 10:155.

Nematbakhsh, S., C. Pei Pei, J. Selamat, N. Nordin, L. H. Idris, and A. F. Abdull Razis. 2021. Molecular regulation of lipogenesis, adipogenesis and fat deposition in chicken. Genes (Basel) 12:414.

Reimand, J., T. Arak, P. Adler, L. Kolberg, S. Reisberg, H. Peterson, and J. Vilo. 2016. g:Profiler-a web server for functional interpretation of gene lists (2016 update). Nucleic Acids Res. 44:W83–W89.

Ren, S., Y. Bian, Y. Hou, Z. Wang, Z. Zuo, Z. Liu, Y. Teng, J. Fu, H. Wang, Y. Xu, Q. Zhang, Y. Chen, and J. Pi. 2021. The roles of NFE2L1 in adipocytes: structural and mechanistic insight from cell and mouse models. Redox Biol. 44:102015.

Shafeghat, M., S. Kazemian, A. Aminorroaya, Z. Aryan, and N. Rezaei. 2022. Toll-like receptor 7 regulates cardiovascular diseases. Int. Immunopharmacol. 113:109390.

Shannon, P., A. Markiel, O. Ozier, N. S. Baliga, J. T. Wang, D. Ramage, N. Amin, B. Schwikowski, and T. Ideker. 2003. Cytoscape: a software environment for integrated models of biomolecular interaction networks. Genome Res. 13:2498–2504.

Stegen, S., T. Bex, C. Vervaet, L. Vanhee, E. Achten, and W. Derave. 2014. β-Alanine dose for maintaining moderately elevated muscle carnosine levels. Med. Sci. Sports Exerc. 46:1426–1432.

Sun, Y., G. Zhao, R. Liu, M. Zheng, Y. Hu, D. Wu, L. Zhang, P. Li, and J. Wen. 2013. The identification of 14 new genes for meat quality traits in chicken using a genome-wide association study. BMC Genomics 14:458.

Szklarczyk, D., R. Kirsch, M. Koutrouli, K. Nastou, F. Mehryary, R. Hachilif, A. L. Gable, T. Fang, N. T. Doncheva, S. Pyysalo, P. Bork, L. J. Jensen, and C. von Mering. 2023. The STRING database in 2023: protein-protein association networks and functional enrichment analyses for any sequenced genome of interest. Nucleic Acids Res. 51:D638–D646.

Tatsuda, K., and K. Fujinaka. 2001. Genetic mapping of the QTL affecting body weight in chickens using a F2 family. Br. Poult. Sci. 42:333–337.

Vandesompele, J., K. De Preter, F. Pattyn, B. Poppe, N. Van Roy, A. De Paepe, and F. Speleman. 2002. Accurate normalization of real-time quantitative RT-PCR data by geometric averaging of multiple internal control genes. Genome Biol. 3 Research0034.

Vera Alvarez, R., L. S. Pongor, L. Mariño-Ramírez, and D. Landsman. 2019. TPMCalculator: one-step software to quantify mRNA abundance of genomic features. Bioinformatics 35:1960–1962.

von Roemeling, C. A., L. A. Marlow, A. B. Pinkerton, A. Crist, J. Miller, H. W. Tun, R. C. Smallridge, and J. A. Copland. 2015. Aberrant lipid metabolism in anaplastic thyroid carcinoma reveals stearoyl CoA desaturase 1 as a novel therapeutic target. J. Clin. Endocrinol. Metab. 100:E697–E709.

Yang, S. H., Y. X. Guo, G. Q. Liu, Y. Q. Liu, and Y. J. Zhang. 2021. Use of a short-term nutritional supplementation for transcriptional profiling of liver tissues in sheep. Small Ruminant Res. 203:106464.

Zhang, F., Q. Xiong, H. Tao, Y. Liu, N. Zhang, X. F. Li, X. J. Suo, Q. P. Yang, and M. X. Chen. 2021. ACOX1, regulated by C/EBPα and miR-25-3p, promotes bovine preadipocyte adipogenesis. J. Mol. Endocrinol. 66:195–205.

Zhang, M., F. Li, X. F. Ma, W. T. Li, R. R. Jiang, R. L. Han, G. X. Li, Y. B. Wang, Z. Y. Li, Y. D. Tian, X. T. Kang, and G. R. Sun. 2019. Identification of differentially expressed genes and pathways between intramuscular and abdominal fat-derived preadipocyte differentiation of chickens in vitro. BMC Genomics 20:743.

Zhang, R., R. Li, Q. Feng, L. Zhi, Z. Li, Y. O. Xu, and Y. Lin. 2018. Expression profiles and associations of FGF1 and FGF10 with intramuscular fat in Tibetan chicken. Br. Poult. Sci. 59:613–617.

Zhang, T., X. Zhang, K. Han, G. Zhang, J. Wang, K. Xie, and Q. Xue. 2017. Genome-wide analysis of lncRNA and mRNA expression during differentiation of abdominal preadipocytes in the chicken. G3 (Bethesda) 7:953–966.

Zhao, G. P., J. L. Chen, M. Q. Zheng, J. Wen, and Y. Zhang. 2007. Correlated responses to selection for increased intramuscular fat in a Chinese quality chicken line. Poult. Sci. 86:2309–2314.

Zheng, H., J. Fu, P. Xue, R. Zhao, J. Dong, D. Liu, M. Yamamoto, Q. Tong, W. Teng, W. Qu, Q. Zhang, M. E. Andersen, and J. Pi. 2015. CNC-bZIP protein Nrf1-dependent regulation of glucose-stimulated insulin secretion. Antioxid. Redox Signal. 22:819–831.

Zhou, Z., D. Cai, G. Wei, B. Cai, S. Kong, M. Ma, J. Zhang, and Q. Nie. 2023. Polymorphisms of CRELD1 and DNAJC30 and their relationship with chicken carcass traits. Poult. Sci. 102:102324.

Zieba, D. A., M. Amstalden, and G. L. Williams. 2005. Regulatory roles of leptin in reproduction and metabolism: a comparative review. Domest. Anim. Endocrinol. 29:166–185.